Rheological Behavior of POSS/Polyurethane−Urea Nanocomposite Films Prepared by Homogeneous Solution Polymerization in Aqueous Dispersions

Samy A. Madbouly,† Joshua U. Otaigbe,* Ajaya K. Nanda, and Douglas A. Wicks

School of Polymers and High Performance Materials, The University of Southern Mississippi, Hattiesburg, Mississippi 39406

Received January 23, 2007; Revised Manuscript Received March 22, 2007

ABSTRACT: Reinforced polyurethane−urea nanocomposite with reactive polyhedral oligomeric silsesquioxanes (POSS) has been prepared via environmentally friendly aqueous dispersion with no organic solvent. Rheological behavior of this important class of materials has been investigated as a function of POSS concentration over a wide range of shear frequency and temperature (−100 to 230 °C). The functionalized diamino-POSS was reacted initially with isophorone diisocyanate (the urethane hard segments) before adding the polyester diol (the soft segments). The complete reaction of diamino-POSS with urethane segments was confirmed rheologically and morphologically (TEM). The molecular relaxations of the hard and soft segments of PU/POSS nanocomposites were investigated using the rectangular torsional mode in the glassy and rubbery states. It was found that the storage elastic modulus increased systematically only in the high-temperature range (i.e., the range of the T_g of the urethane segments) while the modulus did not significantly change at low temperatures corresponding to the range of the T_g of the polyester soft segments. In addition, the rheological behavior of the pure PU in the melt confirmed the existence of microphase separation of the hard and soft segments at 140 °C. The value of the microphase separation temperature (T_{MPS}) was found to be concentration independent when the POSS concentration is ≤6 wt %. For 10 wt % POSS the T_{MPS} shifted by 20 °C to a higher temperature. The viscoelastic material functions (G', G'', and η^*) for pure PU film and samples with POSS ≤6 wt % were found to be well described by the time−temperature superposition (or WLF) principle in the low-temperature range studied (i.e., $T < T_{MPS}$ (140 °C)); at higher temperatures the superposition principle failed to describe the experimental data. For 10 wt % POSS film, the validity of WLF principle was extended up to 160 °C due to the shift of T_{MPS} to higher temperature. The incorporation of POSS to the hard segments of PU produced a more homogeneous structure for the 10 wt % POSS as confirmed by TEM. In addition, the viscosity and activation energy of flow were increased dramatically by adding POSS to PU. The thermal stability of PU under a nitrogen atmosphere did not improve by adding POSS, but it improved slightly when tested in an oxygen atmosphere.

Introduction

Incorporation of a well-defined nanostructured inorganic cluster of polyhedral oligomeric silsesquioxanes (POSS) into a polymer matrix to form special organic/inorganic hybrids represents a new chemical feedstock advancement.[1] This technology merges the properties of fillers with the versatility and precision of synthetic chemistry. The nanoscale size of the special hybrids affords molecular level control of polymer dynamics, surface-bulk properties, and biological function. Reactive POSS belong to a special class of functional nanoscale fillers consisting of an eight-corner, $-(SiO_{1.5})_n$-based cage bearing one or more functional groups.[1−8] POSS has been used as an interesting class of precursors for the synthesis of molecularly designed organic/inorganic hybrids. Nanostructured POSS chemicals bridge the gap between fillers and monomers in offering shrinkage control and reinforcement of polymer chains. When appropriately functionalized they can also bridge the gap between polymers and plasticizers without plasticizer migration. The nanostructured POSS materials afford the modification of surfaces with well-defined inorganic/organic segments and offer an alternative to traditional chemical coupling agents such as silanes. The size of the pendant POSS cage is comparable to the dimensions of the linear polymer, enabling POSS to control the motions of the chains at the molecular level with enhanced physical properties while retaining the processability and mechanical properties of the base resin.

Despite the growing number of scientific and patent literature on POSS and related materials, there are few reported examples of practical and optimal exploitation of POSS.[9−11] Such nanoreinforced polymers lead to significant thermomechanical property enhancements, while simultaneously improving or retaining the material's other physical properties such as optical clarity, mechanical, and processability. Other property enhancements such as gas permeability may also be realized to an extent that depends on the type and concentration of POSS used. Typically, high thermal stability, improved environmental durability in special environments (e.g., exposure to atomic oxygen and fire resistance), and, in some cases, improved mechanical properties (reinforcement) have been reported for POSS-modified polymers.[12−14] Generally, POSS can be incorporated into a polymer matrix by two different methods (i.e., mechanical melt blending as nanofiller particles or by chemical functionalization of one or more functional groups into the corner of the POSS chemical structure). This functional group can react chemically with the polymer matrix to produce the polymer-*graft*-POSS composite. In the case of the mechanical melt blending method, the eight corners of the cage structure of POSS have the same unreactive R groups. When the functionalized POSS is chemically reacted (via covalent bonds)

* To whom all correspondence should be addressed: Tel 601-266-5596; e-mail Joshua.Otaigbe@usm.edu.

† Permanent address: Department of Chemistry, Faculty of Science, Cairo University, Orman-Giza 12613, Egypt.

10.1021/ma070186n CCC: $37.00
Published on Web 06/16/2007

with the polymer matrix, the resulting POSS-modified polymer is more thermally stable and reinforced at the molecular level.[15] These desirable attributes of the POSS-modified polymer is ascribed to the resulting nanocomposite's relatively strong POSS−POSS and POSS−polymer interactions.[16−18]

Recently, POSS has been shown to stratify at the surfaces of polymers, providing unique properties for novel applications. The cagelike structures of POSS have been shown to have excellent thermal stability, and their multiple organic groups control the compatibility with an organic matrix, yielding an inorganic/organic hybrid as already mentioned. A special field is represented by POSS-modified polyurethane−ureas[19,20] (PU) because these polymers encompass a huge number of specialized applications. It is expected that incorporation of small amounts of POSS to PU films can significantly enhance the thermal stability and mechanical properties and present a new class of polymer film materials for special industrial applications where current polymer films are not useable. Further, the POSS-modified PU films may be good model systems for exploring feasibility of new routes for driving inorganic/organic hybrid materials to self-assemble into useful materials. It is therefore essential to understand the structure and rheological behavior of this important class of materials so that they can be rationally engineered during processing to yield new materials with enhanced properties for a number of applications.

Traditionally, PU dispersions are produced in the industry after completing the PU polymerization in a homogeneous solution. This process, widely referred to as the "acetone process" in the polyurethane−urea industries, uses a low boiling point water-miscible organic solvent, such as acetone or methyl ethyl ketone, to carry out the polymerization in a concentrated solution. After dispersion of the polymer solution into water the solvent is recovered for reuse by distillation. Although the process just described is practiced industrially,[21−23] there are very few published studies describing this process in the open literature.[24−30] The advantages of this processing route are readily apparent because the finished polymer is prepared in a highly controlled fashion with characterization and adjustments possible before the dispersion process. An additional benefit comes from having the low boiling point solvent completely removed by distillation after the dispersion to yield a product containing little or no volatile organic content. As previously reported,[31] we used homogeneous solution polymerization (or the "acetone process") to produce polyurethane−urea dispersions with functionalized diamino-POSS with different POSS concentrations. The use of acetone as the initial polymerization solvent allowed for the facile incorporation of diamino functional POSS monomers in a homogeneous reaction environment. After addition of water and removal of the acetone, stable dispersions with unimodal particle sizes were obtained.[31] The incorporation of POSS monomers did not have a significant effect on the dispersion's properties. However, the physical properties of the isolated polymers displayed significant changes with notable increases in the T_g and surface hydrophobicity. These changes were attributed to the incorporation of the POSS residues into the hard segment domains. No evidence of gross phase heterogeneity due to the inclusion of POSS moieties was detected by either thermal characterization or wide-angle X-ray diffraction (WAXD).[31]

The present paper is a continuation to the previous part of this work.[31] The present paper will consider in detail the effects of reacted diamino-POSS on the viscoelastic behavior and morphology of polyurethane−urea films produced from homogeneous solution polymerization (or the "acetone process") as a function of POSS composition, shear frequency, and temperatures. The composition dependence of POSS on the zero shear viscosity will be interpreted on the basis of Krieger−Dougherty, Einstein−Batchelor, and Lecyar model equations reported in the literature. The activation energy of flow as a function of POSS concentration will be calculated from the temperature dependence of the shift factor. In addition, the thermal stability of the PU/POSS nanocomposites will be studied under nitrogen and oxygen atmospheres using TGA measurements. The present study may stimulate a better understanding of the rational incorporation of nanostrucutured chemical feedstocks such as POSS into existing polymer systems to generate new hybrid polymer systems with improved properties, making them widely applicable.

Experimental Section

Materials. Poly(hexylene adipate−isophthalate) polyester diol (Desmophen 1019-55-OH# 55 and Acid# 2) and isophorone diisocyanate (IPDI) (Desmodur-I) were supplied by Bayer Material Science, Pittsburgh, PA. Dimethylolpropionic acid (DMPA), dibutyltin dilaurate (DBTDL), triethylamine (TEA), and 1,4-butanediol (BD) were received from Aldrich Chemical Co. Acetone (99.5%) was received from Fluka, and 3-(2-aminoethyl)amino)propylheptaisobutyl-POSS (diamino-POSS) was provided by Hybrid Plastics, Hattiesburg, MS. All materials were used as received.

Representative PU−POSS Hybrid Synthesis (10 wt % POSS). In a 500 mL round-bottom flask equipped with a nitrogen bubbler, 10.0 g of diamino-POSS (0.021 amine equiv) was dissolved into 125 g of acetone. To this solution 23.0 g of IPDI (0.207 isocyanate equiv) was added dropwise while stirring using a magnetic stirrer at 20 °C. After 20 min, 3 drops of DBTDL were added. After 10 min, the flask was fitted with a mechanical stirrer, a thermocouple controlled heating mantle, and a condenser with nitrogen bubbler and a pipet outlet. The polyester polyol (61.1 g, 0.06 hydroxyl equiv) and DMPA (3.1 g, 0.046 hydroxyl equiv, and 0.023 acid equiv) were charged into the flask, and stirring was continued while the temperature was raised to 60 °C. The isocyanate (NCO) content was monitored during the reaction using the standard dibutylamine back-titration method.[32] Upon reaching the theoretical NCO value, the prepolymer was chain extended with BD (2.6 g, 0.057 hydroxyl equiv) and the reaction continued for 2 h to complete polymerization, yielding the desired polyurethane−urea/POSS copolymer. Last, the polymer was neutralized by the addition of 2.3 g of triethylamine (0.023 equiv) and stirred for 30 min while maintaining the temperature at 55 °C. Formation of the dispersion was accomplished by slowly adding water to the neutralized acetone solution of the polyurethane−urea polymers at 45−50 °C over 30 min with agitation speed of 600 rpm. After stirring for 30 min the reaction mixture was transferred to a rotary evaporator, and the acetone was removed at 35 °C and a partial vacuum of 70 mmHg to afford organic solvent free dispersions with 32 wt % solids. Scheme 1 shows the elementary steps for the synthesis of PU/POSS nanocomposite.

Pure PU Dispersion Synthesis. As a control to our experiments, PU sample preparation without POSS was carried out in a 500 mL round-bottom, four-necked flask with a mechanical stirrer, thermocouple, and a condenser equipped with a nitrogen bubbler and a pipet outlet. To the reactor, 73.3 g of the polyester diol (0.071 hydroxyl equiv) and 3.1 g of DMPA (0.046 hydroxyl equiv, 0.023 acid equiv) were charged. While mixing, 85 g of acetone was added, and stirring was continued until a homogeneous mixture was obtained. IPDI (21.2 g, 0.19 isocyanate equiv) and 3 drops of DBTDL were added dropwise with continued stirring at 60 °C. Upon reaching the theoretical NCO value, the prepolymer was chain extended with BD (2.4 g, 0.053 hydroxyl equiv), and the reaction was allowed to continue for 2 h to complete the polymerization. The final polymer was neutralized by the addition of 2.3 g of triethylamine (0.023 equiv) and stirred for 30 min while maintaining the temperature at 55 °C. The dispersion was accomplished as specified above for 10 wt % POSS.

Scheme 1

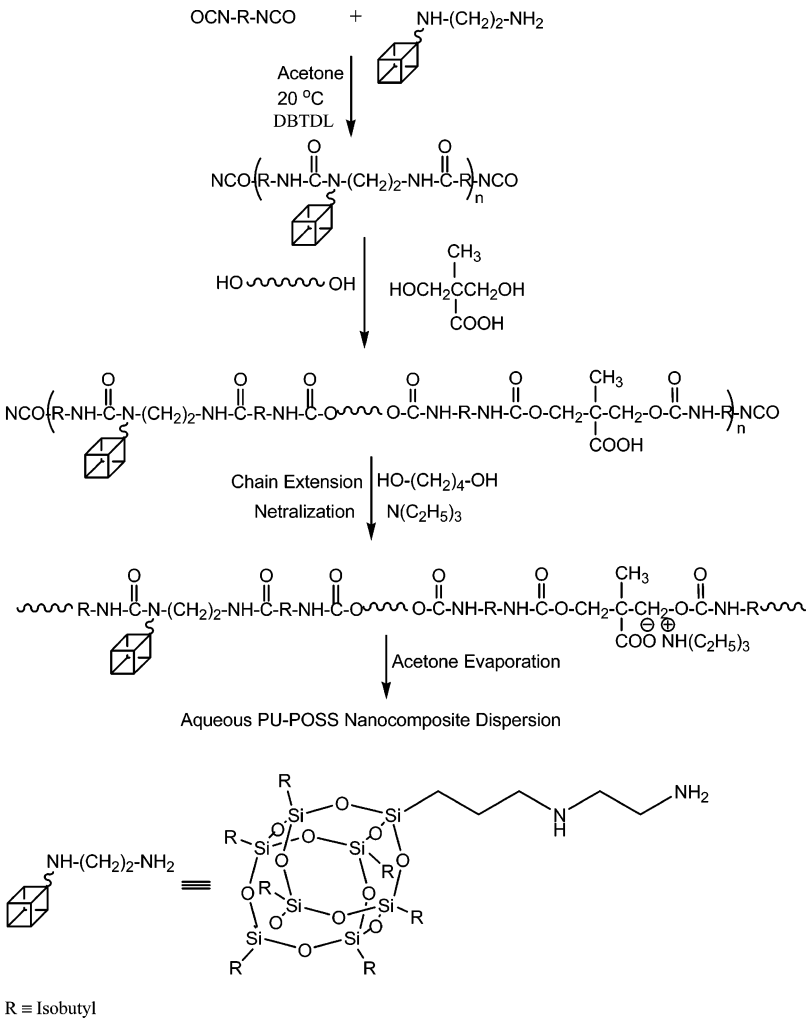

Rheological Measurements. The films of pure PU and PU−POSS nanocomposites with different concentrations were prepared by casting the corresponding dispersions onto a polypropylene plate and drying to constant weight in a vacuum oven at 70 °C for 3 days. The viscoelastic measurements were done on the dried films using an Advanced Rheometerics Expansion System (ARES, TA Instruments) equipped with 25 mm diameter parallel plates. In this study, the following rheological experiments were performed: (1) Strain sweep at a constant temperature and frequency range of 0.1−100 rad/s to obtain the linear viscoelastic range of the dispersions. (2) A time sweep at a constant temperature and frequency to obtain steady state and thus ensure that the measurements were carried out under equilibrium condition. (3) Frequency sweep at a given temperature (100−230 °C) in the linear viscoelastic region (strain amplitude ≤10% strain) to obtain the complex viscosity, $|\eta^*|$, and the dynamic shear moduli, i.e., storage shear modulus, G', and loss modulus, G''. Master curves were obtained by horizontal shifts of the experimental data. The zero shear viscosities (η_0) of the blends were calculated by fitting the $|\eta^*|$ vs ω data to the Carreau−Yasuda model.[33] (4) The viscoelastic behavior of PU/POSS nanocomposites in the glassy and rubbery states (over a wide range of temperature, −100 to 100 °C) was investigated using the torsional rectangular mode (1 mm thick, 5 mm width, and 15 mm length) at 1 rad/s shear frequency and 2 °C/min heating rate.

TEM and TGA Measurements. Samples for transmission electron microscopy (TEM) were prepared by taking a small portion of the hybrid material (approximately 0.5 mm × 0.5 mm) and affixing it onto either a stub or pin holder. The material was frozen to −100 °C, and ultrathin sections were made using a Meager Scientific Reichert Ultracut S ultramicrotome with a FCS cryo-unit and a diatome diamond knife. The sections were collected onto Formvar-coated copper grids using cryoprotectant solution with a wire loop. The cryoprotectant was removed from the sections with distilled water. The grids were then exposed to 0.5% ruthenium tetroxide (RuO_4) in solution by affixing the grids with tape in a glass Petri dish and suspending them over a droplet of the RuO_4 for 2 h. The grids were then imaged using a JEOL 1200 EX II transmission electron microscope at 120 kV. Images were collected using a Megaview III camera and SIS Pro software. The staining step provides electron scattering contrast between the hard and soft segments. RuO_4 is also a good staining agent for POSS.

The thermal stability of PU/POSS nanocomposites was investigated using thermal gravimetric analysis (Pyris Diamond TGA, Perkin-Elmer). The heating rate was 10 °C/min for all measured samples. The measurements were carried out under nitrogen and oxygen atmospheres.

Results and Discussion

This section begins by first investigating the linear viscoelastic behavior of pure PU and subsequently followed by considering the effects of incorporation of small amounts (up to 10 wt %) of reactive nanoscale POSS filler on the rheology, morphology, and thermal stability of the PU matrix.

Pure PU Film. The master curves of the dynamic shear moduli, G' and G'', can be constructed on the basis of the concept of thermorheological simplicity. For example, the storage modulus can be superimposed by horizontal shifts along the *x*-axis (frequency axis), according to the following equation:

$$G'(\omega a_T, T_0) = G'(\omega, T) \quad (1)$$

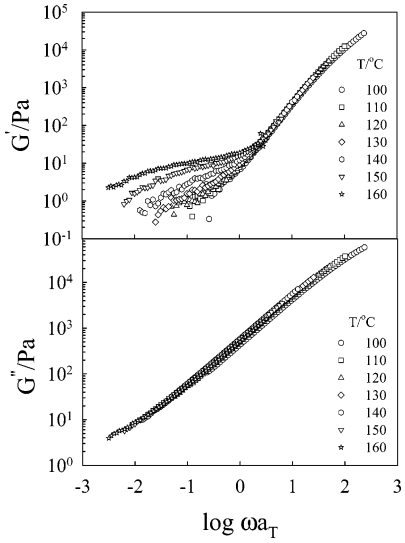

Figure 1. Master curves of the dynamic shear moduli, G' and G'', for pure PU at reference temperature, $T_0 = 120$ °C.

where ω is the magnitude of the shear frequency, a_T is the horizontal shift factor, and T_0 is the reference temperature. The time−temperature superposition principle increases the accessible frequency window of the linear viscoelastic experiments. This principle applies to stable materials without any thermal-induced physical or chemical reactions or transitions during the dynamic measurements, and only the effect of temperature on the relaxation process is considered. Therefore, the principle works well when the stress-sustaining structure in the system does not change with temperature and when the relaxation times of all modes of this structure change with temperature by the same factor. Figure 1 shows the master curves of the dynamic shear moduli, G' and G'', for pure PU sample (0 wt % POSS) at $T_0 = 120$ °C. Clearly there is strong deviation in the terminal zone of the master curve of G' starting at about 140 °C. This deviation means that the WLF (Williams−Landel−Ferry) equation is no longer valid at the high-temperature range. This behavior is attributed to the fact that the PU chemical structure is a multiblock copolymer comprised of alternating soft polyester and hard polyurethane−urea segments. These two segments undergo microphase separation into hard and soft phases, respectively, below and above their glass transition temperatures. This microphase separation is responsible for the excellent elastomeric properties of PU. The G'' does not show any deviation in the terminal zone of the master curve, indicating that the stress induced in the system by the concentration fluctuations accompanying the microphase separation transition is mostly elastic in origin. It is apparent from this figure that the WLF principle is only valid for temperatures lower than 140 °C; the WLF principle failed for $T \geq 140$ °C. The existence of microphase separation transition in PU elastomers has been clearly demonstrated beyond doubt in the literature using different techniques.[34−37] A similar breakdown in the WLF principle has been observed in several diblock and triblock copolymers and polymer blends with lower and upper critical solution temperatures phase diagram (LCST and UCST, respectively). For a number of diblock and triblock copolymer reported in the literature this breakdown of WLF principle has been shown to be related to a microphase separation transition. The microphase separation of PU based on soft segments of polycaprolactone as a function of block length has been investigated rheologically and by using small-angle X-ray scattering (SAXS) measurements by Velankar et al.[37] They

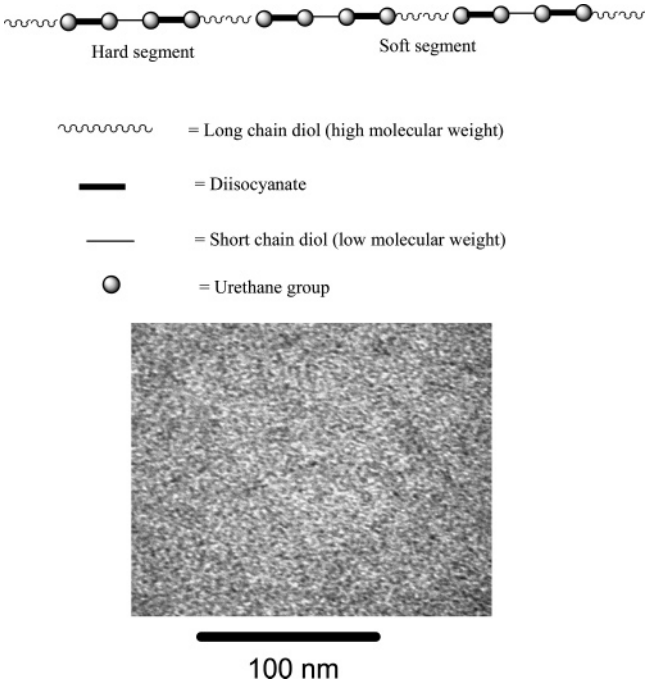

Figure 2. Schematic diagram of the hard and soft segments of PU structure. The TEM shows microphase separation morphology for the hard segments (dark particles) and polyester soft segments (bright matrix).

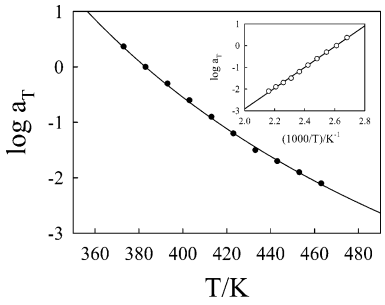

Figure 3. Shift factor a_T as a function of temperature for pure PU. The inset plot demonstrates the Arrhenius-type plot for the temperature dependence of a_T.

showed for the systems studied that the WLF principle failed at high temperatures to an extent that depends on the multiblock lengths.

Figure 2 depicts schematically the structure of PU elastomer as multiblock hard segments (urethane) and soft segments (polyester diol). The TEM shows how these two segments can phase separate into nanoscale morphology. The very small dark particles in the micrograph are the hard segments, and the bright matrix is the soft segments of the PU.

The temperature dependence of the shift factor (a_T) can be studied using the Arrhenius (eq 2) and the WLF (Williams−Landel−Ferry) (eq 3) expressions:[38]

$$\log a_T = \frac{E_A}{2.303R}\left(\frac{1}{T} - \frac{1}{T_0}\right) \tag{2}$$

$$\log a_T = \frac{-c_1(T - T_0)}{c_2 + (T - T_0)} \tag{3}$$

where R is the universal gas constant, E_A is the activation energy of flow, and c_1 and c_2 are the WLF parameters. Figure 3 shows the temperature dependence of the shift factor a_T for the data of Figure 1. The experimental points are fitted by the WLF

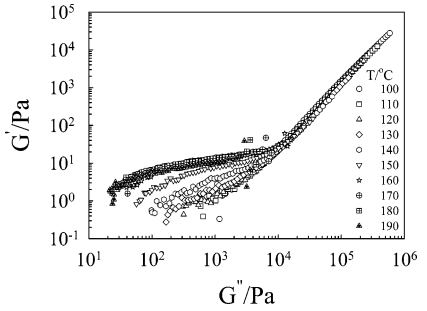

Figure 4. Cole−Cole plot for pure PU at different temperatures.

Equation using c_1 and c_2 as fitting parameters. Although there is a considerable deviation from the master curve of G' at high temperatures in the terminal zone, the temperature dependence of the shift factor is well described by eqs 2 and 3 as shown by the solid lines passing through the experimental data in Figure 3 over the entire temperature range. This experimental fact suggests that the contribution of concentration fluctuations to the viscoelastic material functions caused by microphase separation of the hard and soft segments of PU is not large enough to lead to a considerable deviation from the above two equations. However, these WLF parameters should be taken with extreme caution giving the lack of thermorheological simplicity of the nanocomposite system of this study.

The inset plot of Figure 3 shows the Arrhenius plot for the same experimental data. The value of the E_A obtained from the slope of this straight line is 88 kJ/mol.

An alternative method suggested by Han et al.[39,40] for studying the effect of any thermal-induced transitions, such as order−disorder transition or microphase separation in block copolymers, liquid−liquid transitions (polymer blends), and liquid−solid transitions (gels and crystalline polymers), on the linear viscoelastic properties is to plot G' vs G''. On the basis of this method, only the added contribution of concentration fluctuations caused by those transitions is considered while the frequency and temperature effects are eliminated. This plot is known as a modified Cole−Cole plot (or Han plot) and has been used in the literature for detecting any structure formation caused by thermal-induced transitions in different polymer materials. In the current study the microphase separation of the hard and soft segments of PU can be easily detected, as shown in Figure 4. In the low-temperature range, all curves coincide; however, the curves deviate at high temperatures due to microphase separation. Clearly, the curves start to deviate at 140 °C, indicating that 140 °C is the microphase separation temperature of the hard and soft segments of PU, in good agreement with the value obtained from the deviation in the master curve of G', as shown in Figure 1. The deviation in the curve at the microphase separation temperature is very sharp due to the big difference in the T_gs of the hard and soft segments (i.e., 50 and −50 °C, respectively).

The complex viscosity of PU as a function of angular frequency for different temperatures is shown in Figure 5. Clearly, the viscosity of PU slightly depends on shear frequency and decreases with increasing temperature at low temperatures (T < 140 °C). At T = 140 °C, the viscosity increases slightly in the low shear frequency range and becomes non-Newtonian over a wide frequency range at $T \geq 160$ °C. The dependence of the viscosity of the PU on angular frequency can be expressed through the Carreau−Yasuda model according to the following equation:[33]

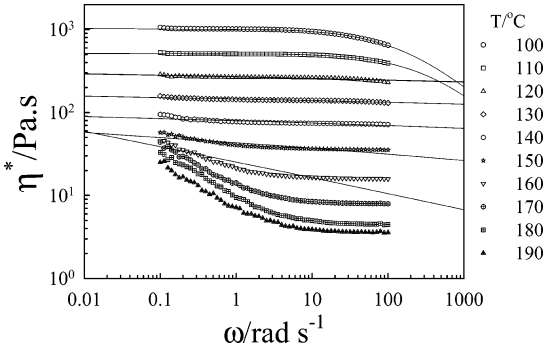

Figure 5. Frequency dependence of dynamic viscosity for pure PU at different temperatures. Solid lines are fits of eq 4 to the experimental data.

$$\eta^* = \eta_0\left[1 + \left(\frac{\eta_0\omega}{\tau^*}\right)^a\right]^{(n-1)/a} \quad (4)$$

where η_0 is the zero-shear viscosity and n, a, and τ^* are material constants. Using the above model, one can calculate η_0 as a fitting parameter to the experimental results using nonlinear regression technique. An excellent description of the data was obtained as shown in Figure 5 at T < 140 °C. At higher temperatures, eq 4 failed to describe the experimental data. Note that in Figure 5 the lines are computed from eq 4, while the symbols are experimental data. The value of zero shear viscosity calculated from this fitting as a function of temperature is considered with other PU−POSS composites in the next section.

PU−POSS Nanocomposites. The master curves of the dynamic shear moduli, G' and G'', for PU/POSS nanocomposite with 10 wt % POSS are shown in Figure 6. Similar to Figure 1, there is a considerable deviation in the terminal zone of the master curve of G' only in the high-temperature range. As before, this deviation indicates failure of the WLF equation to describe the viscoelastic behavior of both PU and PU−POSS at high temperatures due to the microphase separation of the hard and soft segments. It is also clear from this figure that the incorporation of reactive POSS to the PU chains can significantly affect the microphase separation temperature as evidenced by the reduced deviation in the terminal zone compared to that of pure PU already described. In addition, the G' starts to deviate from the master curve at 160 °C, which is 20 °C higher than that of pure PU as shown in Figure 1. This experimental fact suggests that the incorporation of small amounts of nanoscale POSS to the hard segments of PU enhances the miscibility between the hard and soft segments, producing relatively more homogeneous composite at elevated temperatures. This enhancement in the miscibility and phase homogeneity is confirmed by TEM investigation, as will be discussed later.

The inset plot of Figure 6 shows the temperature dependence of shift factor used to construct the master curves of G' and G'' for PU/POSS (10 wt % POSS). The experimental data (symbols) were found to be well described by the WLF principle (eq 3) even though the shifts did not produce a good superpositioning of G' at high temperatures due to the microphase separation transition, as already mentioned. The shift factor as a function of temperature was also found to be consistent with the Arrhenius equation (2), as depicted in the inset plot of Figure 7. The activation energy of flow for the PU/POSS with 10 wt % POSS obtained from the slope of the straight line of Figure 7 is about 138 kJ/mol, a value much higher than that calculated for the pure PU (88 kJ/mol). The inset plot of Figure 7 demonstrates the composition dependence of POSS on the

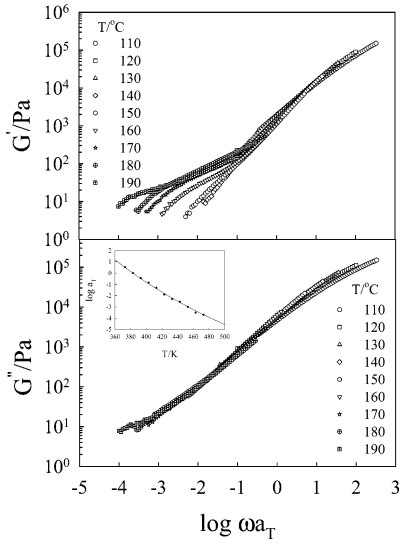

Figure 6. Master curves of the dynamic shear moduli, G' and G'', for PU/POSS composite with 10 wt % POSS at reference temperature, $T_0 = 120$ °C. The inset plot represents the shift factor a_T as a function of temperature (the solid line is calculated from eq 3).

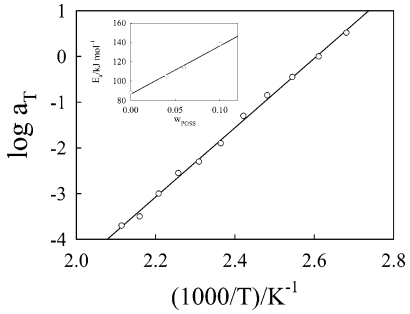

Figure 7. Arrhenius-type plot for the temperature dependence of a_T for PU/POSS (10 wt % POSS). The inset plot shows POSS concentration dependence of the activation energy of flow for PU/POSS nanocomposites.

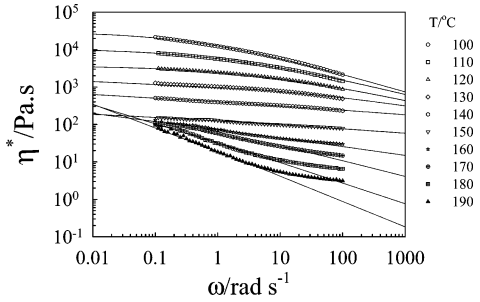

Figure 8. Frequency dependence of dynamic shear viscosity for PU/POSS composite (10 wt % POSS) at different temperatures. Solid lines are fits of eq 4 to the experimental data.

activation energy of flow for PU/POSS nanocomposite. Clearly, the activation energy increase linearly with increasing POSS concentration. On the basis of this experimental fact, one can say that the incorporation of POSS nanofiller to the polymer chains of PU can increase the phase homogeneity of the hard and soft segments, producing more homogeneous materials with high temperature-dependent viscosities.

The complex viscosity of PU with 10 wt % POSS as a function of shear frequency at different constant temperatures is shown in Figure 8. The absolute value of η^* is about $1^1/_2$ orders of magnitude higher than that of pure PU at identical temperature and shear frequency (Figure 5). The lines in Figure 8 are computed from eq 4, and the symbols are experimental

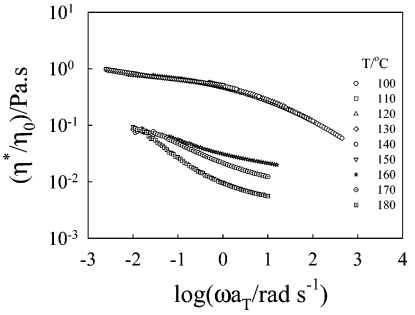

Figure 9. Master curve of normalized viscosity, η^*/η_0 at $T_0 = 120$ °C for PU/POSS composite (10 wt % POSS).

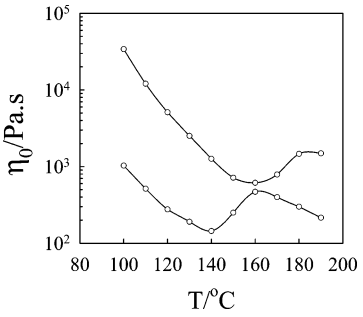

Figure 10. Temperature dependence of the zero shear viscosity for pure PU and PU/POSS nanocomposite (10 wt % POSS).

data. Similar to the behavior of pure PU, the viscosity increases at high temperatures ($T \geq 160$ °C), especially at low shear frequency due to the microphase separation of the hard and soft segments. The composition and temperature dependencies of zero shear viscosity and its relationship to the microphase separation transition will be considered later.

The master curve of the dynamic shear viscosity can be obtained by considering the most current theories that attempt to describe the flow behavior of polymers using expressions of the type[41]

$$\eta^*/\eta_0 = f(a_T\omega) \tag{5}$$

Here, $f(a_T\omega)$ is assumed to be a universal function that is independent of molecular weight, concentration, and temperature. From eq 5 it is apparent that the parameter η_0 is very important in calculating the master curve. The values of η_0 at different temperatures were accurately evaluated by fitting the classical frequency dependence of complex dynamic viscosity to eq 4, as already described. A satisfactory master curve for PU/POSS nanocomposite containing 10 wt % POSS was obtained at temperatures lower than that obtained at the microphase separation temperature, as shown in Figure 9. At temperatures higher than the microphase separation temperature, eq 5 is no longer applicable, and a clear deviation from the master curve can be observed as Figure 9 shows. This deviation in the master curve is attributed to the influence of an excess viscosity caused by concentration fluctuations that must be taken into account for accurate interpretation of the data. In addition, the increase in the viscosity at high temperatures and at low shear frequency leads to an increase in the zero shear viscosity value, and consequently, the reduced viscosity (η^*/η_0) will decrease significantly, producing more obvious deviation of the experimental data from the master curve.

The calculated values of η_0 at different temperatures based on eq 4 for pure PU and PU/POSS with 10 wt % POSS (Figures 5 and 8, respectively) is shown in Figure 10. Clearly, this figure shows that η_0 decreases with temperature in the low-temperature

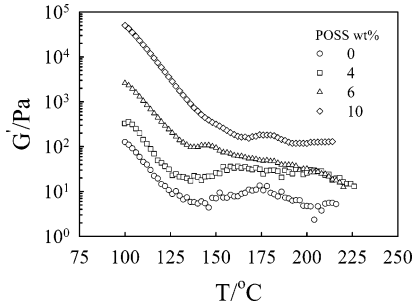

Figure 11. Temperature dependence of the storage modulus of PU/POSS nanocomposites for different POSS concentrations at 1 rad/s shear frequency and 2 °C/min heating rate.

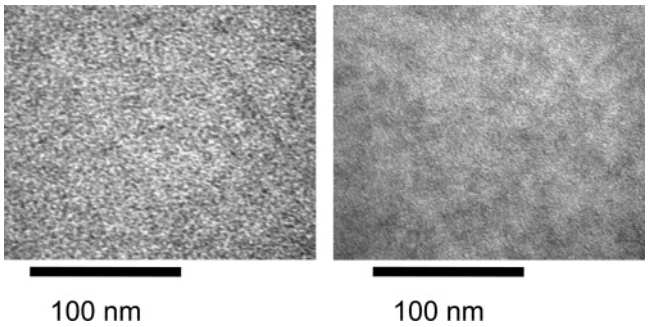

Figure 12. TEM photographs for pure PU and PU/POSS composite (10 wt % POSS). The dark particles represent the hard segments, and the bright matrix represents the polyester soft segments. The sample of 10 wt % POSS shows finer morphology than that of pure PU.

range due to the increase in mobility of the polymer chains caused by Brownian motion. At the microphase separation temperature, a considerable change in the slope of η_0 was observed. It is apparent that the change of η_0 at the phase separation temperature might be attributed to a competition between two opposing factors. One factor tends to decrease η_0 with increasing temperature due to Brownian motion, and the other factor is the concentration fluctuations at the microphase separation temperature that gives rise to an additional contribution to η_0.[42−45] The value of the microphase separation temperature (T_{MPS}) can be obtained from the onset temperature at which the slope of η_0 vs T starts to deviate. Based on this method, the T_{MPS} of pure PU and PU/POSS composite (10 wt % POSS) is 140 and 160 °C, respectively. This observation supports our suggestion that POSS can enhance the miscibility of the hard and soft segments of PU to produce a relatively more homogeneous nanoscale morphology, as will be confirmed by TEM investigations described later. A similar behavior was also seen in the dynamic heating ramps (2 °C/min heating rate at $\omega = 1$ rad/s) of the viscoelastic material functions such as G', as shown in Figure 11 for pure PU and PU/POSS nanocomposites of different POSS concentrations. The value of G' is observed to be very sensitive to the phase separation temperatures. Both the temperature dependencies of η_0 (Figure 10) and G' (Figure 11) give the same values of the microphase separation temperatures (T_{MPS}). It is also very clear from these figures that the value of T_{MPS} is relatively unaffected by POSS concentrations up to 6 wt % POSS. At 10 wt % POSS the T_{MPS} increased by about 20 °C, as shown in Figures 10 and 11. Therefore, the morphology of this PU/POSS with 10 wt % POSS is considered below to get deeper understanding of the structure/property relationships in this important class of material.

Figure 12 shows a comparison between the TEM photograph of pure PU and PU/POSS with 10 wt % POSS. The other concentrations (POSS ≤ 6 wt %) have almost similar morphologies to that of pure PU (not shown). It is clearly evident from this figure that the morphology of PU/POSS with 10 wt % POSS does not show any segregation or aggregation of POSS particles, but it shows a finer structure compared to that of pure PU. This experimental evidence indicates that the diamino-POSS is completely chemically reacted with the hard segments and that the incorporation of POSS in the molecular chains of PU enhances the miscibility between these incompatible hard and soft segments to produce a more homogeneous structure.

The large surface area of the POSS nanoparticles that creates a large interaction zone with the PU segments is thought to be the major reason for the high miscibility of the PU hard and soft segments. It is well established in the literature that the high surface area of nanoparticles leads to a large volume fraction of the polymer matrix, which in turn leads to different bulk properties of the polymer nanocomposite that is enhanced by the interaction zone. Depending on the degree of the interaction between the polymer and nanoparticles, this interaction region can have a higher or lower mobility than that of the bulk material.[46,47] The large surface area can lead to changes in the morphology of the polymers as reported in the literature.[46,47]

In the current PU/POSS system, the total free energy should include the interaction parameters of POSS with the PU hard and soft segments. The POSS/PU mixture can form a thermodynamically stable system when the Gibbs free energy of mixing is negative (i.e., $\Delta G_{mix} < 0$) as a consequence of the interactions of the POSS with both of the hard and soft segments of the PU backbone. In this context, two possible distinct situations can be envisaged. First, the POSS nanoparticles may have favorable interactions with the PU hard and soft segments, leading to a negative value of ΔG_{mix}. In this case, the mixture should be miscible without any phase separation. Second, the POSS may have strong interactions with one segment and weak interactions with the other segment of the PU. In this case, the system may show either an increase in viscosity or a shift in the critical point to an extent that depends on the specific composition of the system and the relative degree of the interaction parameters. On the basis of the TEM morphologies presented in Figure 12, it is apparent that the incorporation of POSS can induce a more miscible structure between the hard and soft segments of PU. While this experimental fact is attributed to the interactions of POSS with the PU hard and soft segments, it is noteworthy that the degree of interactions is not sufficient to produce a completely miscible system like other researchers have reported for other polymer nanocomposites. For example, a number of researchers have reported that organoclays can effectively reduce the domain size of immiscible polymer blends.[48−53] This observation just mentioned was attributed to the clay acting as a physical barrier that slows down the coalescence of the dispersed phases through pinning or increasing viscosity of the system. Very recently, Si et al.[54] reported the morphology of blends of PS/PMMA, PC/SAN24, and PMMA/EVA with modified organoclays (Closite 20A and Cloisite 6A). The authors just mentioned found a large reduction in domain sizes and the localization of the clay platelets along the interfaces of the two components. It is noteworthy that our results and that of prior work reported by others on somewhat similar polymer nanocomposites are consistent with the expectation of POSS-induced enhancement in the miscibility of the PU hard and soft segments and with the observed consequent improvement in the phase homogeneity. As already discussed, these experimental facts can be ascribed to the large surface area of the nanoparticle producing relatively large interaction zones with the PU hard

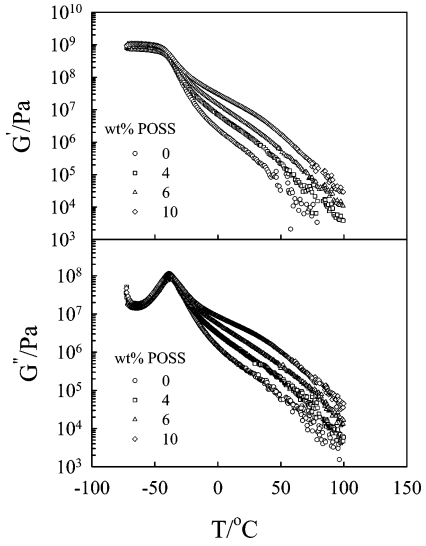

Figure 13. Temperature dependence of the dynamic shear moduli, G' and G'', of PU/POSS nanocomposites for different POSS concentrations at 1 rad/s shear frequency and 2 °C/min heating rate.

and soft segments.

As already described in the Experimental Section, the POSS is initially reacted with the diisocyanates (hard segments) prior to addition of the polyester polyol. Therefore, it is expected that the hard segments of PU will be more affected by the presence of POSS than the soft segments. To confirm this hypothesis experimentally, the viscoelastic measurements of PU/POSS nanocomposites were investigated in the glassy and rubbery states (over a wide range of temperature, −100 to 100 °C) using the torsional rectangular configuration at shear frequency of 1 rad/s and 2 °C/min heating rate. The temperature dependence of G' for PU and PU/POSS composites of different concentrations of POSS is shown in Figure 13. One can see a significant effect of POSS on the molecular relaxations of the hard segments of PU. However, the molecular relaxations of the soft segments remained constant and independent of the concentrations of POSS. The systematic increase in the elastic storage modulus with increasing POSS concentrations at elevated temperatures is attributed to the increase in the T_g of the hard segments.[31] This result suggests that POSS is completely reacted with the hard segments without producing any effect on the soft segments as expected. The increase in the T_g of the hard segment with increasing POSS concentration has been confirmed by DSC measurements in a prior companion publication to the current article.[31]

Effect of POSS Concentration on Zero Shear Viscosity and Thermal Stability. The complex viscosity of pure PU and PU/POSS as a function of angular frequency for different concentrations of POSS at 110 °C is shown in Figure 14. We selected $T = 110$ °C for this comparison because it is lower than the T_{MPS} of all samples. The viscosity of PU changed greatly with increasing concentration of POSS (i.e., the higher the concentration of POSS, the larger the increase in the complex viscosity). The viscosity increased by more than $1^1/_2$ orders of magnitude for PU/POSS with 10 wt % POSS and exhibits more non-Newtonian behavior over the entire range of shear frequency compared to that of pure PU at the same temperature (see Figure 14). The lines passing through the experimental data were calculated using eq 4, as already described. Figure 15a illustrates the volume fraction (ϕ) dependence of the dimensionless viscosity of the PU/POSS nanocomposites, η_r (reduced by the viscosity of pure PU). The critical volume fraction of POSS

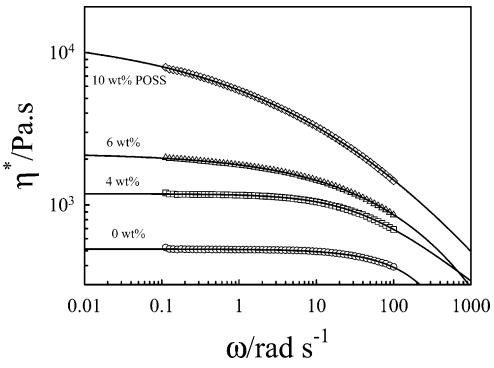

Figure 14. Angular frequency dependence of complex viscosity for PU/POSS nanocomposites of different POSS concentrations at 110 °C. The solid lines are calculated from eq 4 using the nonlinear regression technique.

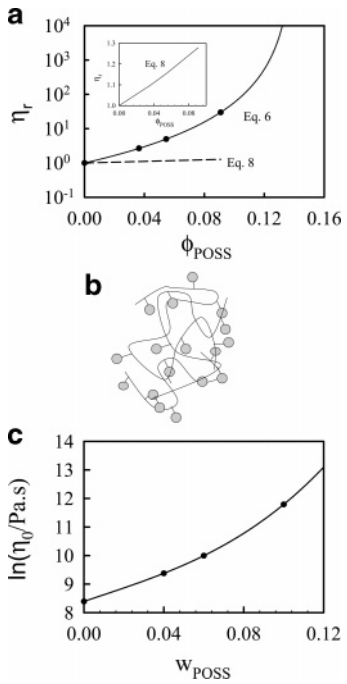

Figure 15. (a) Reduced-zero shear viscosity as a function of volume fraction of POSS at 110 °C for PU/POSS nanocomposites. The solid and dotted lines are given by Krieger−Dougherty and Einstein−Batchelor equations, respectively. The inset plot shows the elevation of reduced-zero shear viscosity by adding Nan filler to PU matrix using the Einstein−Batchelor equation (eq 8). (b) Schematic diagram of a typical PU/POSS nanocomposite. (c) Zero shear viscosity as a function of weight fraction of POSS at 110 °C for PU/POSS nanocomposites. The solid line is calculated from the Lecyar model (eq 9).

(ϕ_c) at which the viscosity of the composite increased strongly was determined using the Krieger−Dougherty equation:[55]

$$\eta_r = \left(1 - \frac{\phi}{\phi_c}\right)^{-k\phi_c} \tag{6}$$

with

$$\eta_r = \frac{\eta_0(\phi)}{\eta_0(0)} \tag{7}$$

where k is a shape parameter, $\eta_0(\phi)$ is the zero shear viscosity of the composites, and $\eta_0(0)$ is the zero shear viscosity of pure PU. The experimental data can be described using the above equation, where the symbols are experimental data while the line is the calculated line using k and ϕ_c as fitting parameters.

The value of ϕ_c obtained from this regression analysis was found to be 0.14. The Krieger−Dougherty equation works well for hard-sphere dispersions with volume fraction less than 0.55. It is well-known that the value of ϕ_c strongly depends on the specific system under consideration. For example small, monodispersed samples show lower value of ϕ_c than large ones, and ϕ_c increases with polydispersity.[56] Clearly, Figure 15a shows an excellent description of the experimental data using eq 6. The Einstein or the modified Einstein−Batchelor equation (eq 8)[57] for hard-sphere suspensions shown by the dotted line in Figure 15a is clearly deviated from the experimental data. Normally, the Einstein−Batchelor equation predicts a slight increase in the zero shear viscosity for suspensions of hard-sphere particles in a polymer matrix.[57]

$$\eta_0(\phi) = \eta_0(0)\{1 + 2.5\phi + 6.2\phi^2 + ...\} \qquad (8)$$

The value of reduced viscosity as a function of volume fraction calculated from the Einstein−Batchelor equation is shown in the inset plot of Figure 15a. Clearly, the magnitude of the elevation in the reduced zero shear viscosity caused by the hard-sphere particles is very small compared to the actual increase in viscosity in the present system (PU/POSS).

Although the empirical Krieger−Dougherty equation works well for this system, it is well-established that this equation is traditionally applied to hard-sphere dispersions. Here, the Krieger−Dougherty equation is used for the current PU/POSS system because of the fact that POSS molecules can be thought of as the smallest particles of silica possible.[58] The chemical structure of POSS is an inorganic/organic hybrid that is intermediate ($RSiO_{1.5}$) between that of silica (SiO_2) and silicone (R_2SiO). However, unlike pure silica or modified clays, each POSS molecule contains covalently bonded reactive functionalities suitable for polymerization or grafting POSS monomers to polymer chains. In fact, POSS is reported in the literature to form spherical particles with 1.5 nm diameter, and its inorganic/organic hybrid nature makes it reasonable to conceptually think of them as hard spheres in contrast to the relatively soft PU chains. Therefore, by copolymerizing or grafting POSS with PU, the POSS can be conjectured to preserve its spherical shape, as schematically depicted in Figure 15b. The above hypothesis is supported by the fact that the experimental data is well described by the Krieger−Dougherty equation, as illustrated by Figure 15a. Further, it is worthy to note that the Krieger−Dougherty equation has been used by a number of researchers in the literature to describe the viscosity of nonspherical or highly charged particles where the parameter ϕ_c (or maximum packing fraction) is a function of particle shape, particle size distribution, and shear rate.

However, in the current PU/POSS system the POSS is completely reacted with the hard segments of PU, and there is no unreacted dispersed phase in this nanocomposite as confirmed by the TEM. Therefore, the current system is a homogeneous composite containing POSS that is completely reacted with the hard segments (urethane segments) to form part of the PU main chain. Therefore, it is reasonable to examine the composition dependence of zero shear viscosity of this composite using another model for miscible polymer mixtures, such as the Lecyar model described by the following equation:[59]

$$\ln \eta_b = Aw_1^3 + Bw_2^3 + Cw_1^2w_2 + Dw_1w_2^2 \qquad (9)$$

where w_1 and w_2 are the weight fractions of PU and POSS, respectively. The constants *A, B, C,* and *D* are material parameters that are both functions of shear frequency and temperature. A slightly negative deviation from the linear mixing rule ($\ln \eta_b = w_1 \ln \eta_1 + w_2 \ln \eta_2$, where η_1 and η_2 are the zero shear viscosity of PU and POSS, respectively) was detected for this nanocomposite, as clearly seen in Figure 15c. The line is computed from eq 9 using a nonlinear regression method, while the symbols are experimental data; a good description of the data was obtained using this model. This equation is normally used to describe the composition dependence of shear viscosity of miscible polymer blends. Recently, we reported a negative deviation from the additivity rule in miscible polymer blend of poly(methyl methacrylate)/poly(methylstyrene-*co*-acrylonitrile), and the data were well described by the Lecyar model.[60] It is noteworthy that this is not a general behavior for all miscible polymer mixtures. To our knowledge, there is no generally acceptable and universal valid mixing rule for the viscosity of polymer mixtures.[61]

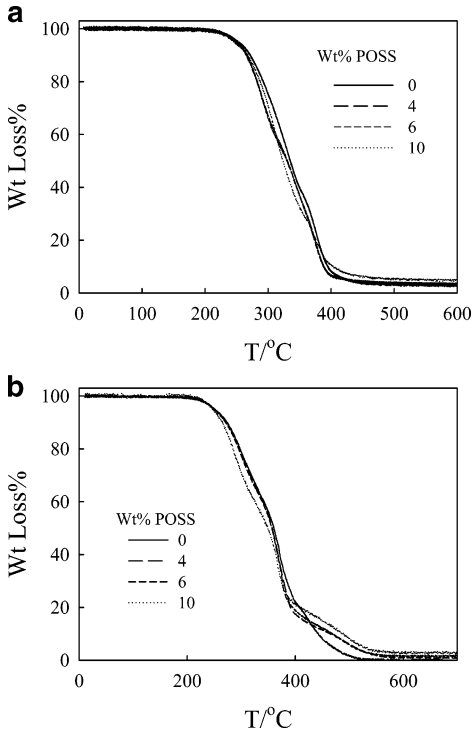

Figure 16. (a) TGA measurements for PU/POSS nanocomposites of different POSS concentrations at 10 °C/min heating rate under a nitrogen atmosphere. (b) TGA measurements for PU/POSS nanocomposites of different POSS concentration at 10 °C/min heating rate under an oxygen atmosphere.

Figure 16a shows the TGA measurements for pure PU and PU/POSS composites of different POSS concentrations. This figure shows the percent mass loss as a function of temperature at 10 °C/min heating rate under a nitrogen atmosphere. Obviously, the PU and PU/POSS nanocomposites undergo thermal degradation beginning at 270 °C regardless of the concentration of POSS. It is also clear from this figure that the soft segments of PU start to degrade first at 270 °C and the hard segments degrades later on at 350 °C. This figure suggests that the incorporation of POSS to the hard segments of PU does not significantly enhance the thermal stability of PU under a nitrogen atmosphere. Figure 16b shows the same data obtained under an oxygen atmosphere. Clearly, the PU/POSS nanocomposite with 10 wt % POSS becomes more thermally stable at high temperature. For example, at 510 °C PU is completely degraded without any inert residue remaining. In contrast, there is more than 15% of PU/POSS (10 wt % POSS) present at this temperature. At temperatures higher than 550 °C, about 5 wt

% inert residue remains for PU/POSS with 10 wt % POSS.

Conclusions

The viscoelastic behavior of polyurethane−urea film changed greatly by incorporation of small amounts (up to 10 wt %) of functionalized diamino-polyhedral oligomeric silsesquioxanes (POSS). A significant increase in the melt viscosity and zero shear viscosity was observed. This increase in the viscosity is attributed to the reaction between the hard segments of PU (urethane segments) and diamino-POSS as confirmed by the increase in the storage modulus with increasing concentration of POSS only at the high-temperature range of the hard segments with no change in the low-temperature range of the soft segments. The viscoelastic data in the melt state confirmed the existence of microphase separation transition, T_{MPS}, of the hard and soft segments at about 140 °C for pure PU. For samples containing POSS ≤ 6 wt %, the value of T_{MPS} was found to be concentration independent; i.e., the T_{MPS} remains constant at 140 °C regardless of the different concentrations of POSS. The T_{MPS} shifted to higher temperature (T_{MPS} = 160 °C) for the 10 wt % POSS nanocomposite. This experimental fact suggest that the incorporation of diamino-POSS to the hard segments of PU enhances their miscibility, producing a more homogeneous structure as confirmed by the TEM (i.e., finer nanoscale morphology was observed for 10 wt % POSS composite compared to that of pure PU). Only one master curve for both G' and G'' can be constructed at a temperature range lower than the T_{MPS}. At higher temperatures a strong deviation from the master curve at the terminal zone of G' was observed, and the WLF superposition principle was no longer valid in this temperature zone. In addition, the incorporation of POSS produces nanocomposites with viscosities of high temperature dependence as confirmed by the linear increase in the activation energy of flow with increasing concentration of POSS. Furthermore, POSS does not seem to enhance the thermal stability of PU under a nitrogen atmosphere; however, a slight improvement in the thermal stability was observed under an oxygen atmosphere. Overall, the results of the present study confirm that homogeneous dispersion of POSS in polyurethane−ureas can be reliably probed by rheological and TEM methods and that the sequencing of the reaction steps previously reported in detail elsewhere[31] dictates the quality of POSS dispersion, making it possible to prepare nanostructured PU/POSS films with prescribed morphology and physical properties.

Acknowledgment. This work was primarily supported by the National Science Foundation MRSEC (DMR 0213883) and in part by the Robert M. Hearin Support Foundation and Bayer MaterialScience, Pittsburgh, PA. The research work of J.U.O.'s former graduate students and postdocs is gratefully acknowledged.

References and Notes

(1) POSS is a Trademark of Hybrid Plastics (www.hybridplastics.com).
(2) Lichtenhan, J. D. *Comments Inorg. Chem.* **1995**, *17*, 115.
(3) Schwab, J. J.; Lichtenhan, J. D. *Appl. Organomet. Chem.* **1998**, *32*, 707.
(4) Laine, R. M.; Zhang, C.; Sellinger, A.; Viculis, L. *Appl. Organomet. Chem.* **1998**, *12*, 715.
(5) Lucke, S.; Stopperk-Langner, K. *Appl. Surf. Sci.* **1999**, *145*, 713.
(6) Shockey, E. G.; Bolf, A. G.; Jones, F.; Schwab, J. J.; Chaffee, K. P.; Haddad, T. S.; Lichtenhan, J. D. *Appl. Organomet. Chem.* **1999**, *13*, 311.
(7) Li, G.; Wang, L.; Ni, H.; Pittman, C. U. J. *Inorg. Organomet. Polym.* **2002**, *11*, 123.
(8) Schmidt, D.; Shah, D.; Giannelis, E. P. *Curr. Opin. Solid State Mater. Sci.* **2002**, *6*, 205.
(9) Gilman, J. W.; Schlitzer, D. S.; Lichtenhan, J. D. *J. Appl. Polym. Sci.* **1996**, *60*, 591.
(10) Phillips, S.; Haddad, T. S.; Tomczak, S. J. *Curr. Opin. Solid State Mater. Sci.* **2004**, *8*, 21.
(11) Gonzalez, R. I.; Phillips, S.; Hoflund, G. B. *J. Spacecr. Rockets* **2000**, *37*, 463.
(12) Gao, F.; Tong, Y.; Schricker, S. R.; Culbertson, B. M. *Polym. Adv. Technol.* **2001**, *12*, 355.
(13) Tegou, E.; Bellas, V.; Gogolides, E.; Argitis, P. *Microelectron. Eng.* **2004**, *238*, 73−74.
(14) Kickelbick, G. *Prog. Polym. Sci.* **2003**, *28*, 83.
(15) Lichtenhan, J. D.; Vu, N. Q.; Carter, J. A.; Gilman, J. W.; Feher, F. J. *Macromolecules* **1993**, *36*, 2141.
(16) Lichtenhan, J. D.; Otonari, Y. A. *Macromolecules* **1995**, *28*, 8435.
(17) Tsuchida, A.; Bolln, C.; Sernetz, F. G.; Frey, H.; Muelhaupt, R. *Macromolecules* **1997**, *30*, 2818.
(18) Mather, P. T.; Jeon Hong, A.; Romo-Uribe, A.; Haddad, T. S.; Lichtenhan, J. D. *Macromolecules* **1999**, *32*, 1194.
(19) Neumann, D.; Fisher, M.; Tran, L.; Matisons, J. G. *J. Am. Chem. Soc.* **2002**, *124*, 13998.
(20) Turri, S.; Levi, M. *Macromolecules* **1999**, *32*, 1194.
(21) Dieterich, D. *Prog. Org. Coat.* **1981**, *9*, 298.
(22) Tirpark, R. L.; Markusch, P. H. *J. Coat. Technol.* **1986**, *58*, 49.
(23) Wicks, Z. W., Jr., Jones, F. N., Pappas, S. P. *Organic Coatings: Science and Technology*; Wiley: New York, 1992; Vol. 1.
(24) Yang, C. H.; Lin, S. M.; Wen, T. C. *Polym. Eng. Sci.* **1995**, *35*, 722.
(25) Wen, T. C.; Wu, M. S.; Yang, C. H. *Macromolecules* **1999**, *32*, 2712.
(26) Wen, T. C.; Wang, Y. J.; Cheng, T. T.; Yang, C. H. *Polymer* **1999**, *40*, 3979.
(27) Yang, C. H.; Yang, H. J.; Wen, T. C.; Wu, M. S.; Chang, J. S. *Polymer* **1999**, *40*, 871.
(28) Barni, A.; Levi, M. *J. Appl. Polym. Sci.* **2003**, *88*, 716.
(29) Chinwanitcharoen, C.; Kanoh, S.; Yamada, T.; Hayashi, S.; Sugano, S. *J. Appl. Polym. Sci.* **2004**, *91*, 3455.
(30) Nanda, A. K.; Wicks, D. A. *Polymer* **2006**, *47*, 1805.
(31) Nanda, A. K.; Wicks, D. A.; Madbouly, S. A.; Otaigbe, J. U. *Macromolecules* **2006**, *39*, 7037.
(32) Nanda, A. K.; Wicks, D. A. *Polymer* **2006**, *47*, 1805.
(33) Carreau, P. J.; De Kee, D.; Chhabra, R. P. *Rheology of Polymeric Systems: Principles and Applications*; Hanser: Munich, 1997.
(34) Koberstein, J. T.; Russell, T. P. *Macromolecules* **1986**, *19*, 714.
(35) Ryan, A. J.; Macosko, C. W.; Bras, W. *Macromolecules* **1992**, *25*, 6277.
(36) Wilkes, G. L.; Emerson, J. A. *J. Appl. Phys.* **1976**, *47*, 4261.
(37) Velankar, S.; Cooper, S. L. *Macromolecules* **1998**, *31*, 9181.
(38) Eckstein, A.; Suhm, J.; Friedrich, C.; Maier, R. D.; Sassmannshausen, J.; Bochmann, M.; Mulhaupt, R. *Macromolecules* **1998**, *31*, 1335.
(39) Han, C. D.; Yang, H. H. *J. Appl. Polym. Sci.* **1987**, *33*, 1199.
(40) Han, C. D.; Chuang, H. K. *J. Appl. Polym. Sci.* **1985**, *30*, 4431.
(41) Chee, K. K. *Aspects Polym. Melt Rheol. Abs. Int. B* **1974**, *34*, 59378.
(42) Bates, F. S. *Macromolecules* **1984**, *17*, 2607.
(43) Rosedale, J. H.; Bates, F. S. *Macromolecules* **1990**, *23*, 2329.
(44) Fredrickson, G. H.; Larson, R. G. *Macromolecules* **1987**, *20*, 1897.
(45) Fredrickson, G. H. *J. Chem. Phys.* **1986**, *85*, 5306.
(46) Ash, B. J.; Schadler, L. S.; Siegel, R. W. *J. Polym. Sci., Part B: Phys.* **2004**, *42*, 4371−4383. See also: Ma, D.; Schadler, L. S.; Siegel, R. W.; Hong, J.-I.; Martensson, E.; Onneby, C. *J. Mater. Res.* **2003**, *19*, 3.
(47) Rawal, A.; Urman, K.; Otaigbe, J. U.; Schmidt-Rohr, K. *Chem. Mater.* **2006**, *18*, 6333.
(48) Khatua, B. B.; Lee, D. J.; Kim, H. Y.; Kim, J. K. *Macromolecules* **2004**, *37*, 2454.
(49) Li, Y.; Shimizu, H. *Polymer* **2004**, *45*, 7381.
(50) Yoo, Y.; Park, C.; Lee, S.; Choi, K.; Kim, S.; Lee, J. H. *Macromol. Chem. Phys.* **2005**, *206*, 878.
(51) Li, Y.; Shimizu, H. *Macromol. Rapid Commun.* **2005**, *26*, 710.
(52) Ray, S. S.; Pouliot, S.; Bousmina, M.; Utracki, L. A. *Polymer* **2004**, *45*, 8403.
(53) Ray, S. S.; Bousmina, M. *Macromol. Rapid Commun.* **2005**, *26*, 1639.
(54) Si, M.; Araki, T.; Ade, H.: Kilcoyne, A. L. D.; Fisher, R.; Sokolov, J. C.; Rafailovich, M. H. *Macromolecules* **2006**, *39*, 4793.
(55) Krieger, I. M.; Dougherty, T. J. *Trans. Soc. Rheol. III* **1959**, 137.
(56) Farris, R. J. *Trans. Soc. Rheol. III* **1968**, *2*, 281.
(57) Batchelor, G. K. *J. Fluid Mech.* **1977,** *83*, 97.
(58) Pielichowski, K.; Juguna, J. N.; Janowski, B.; Pielochowski, J. *Adv. Polym. Sci.* **2006**, *201*, 225−296 and references therein. See also: Baney, R. H.; Itoh, M.; Sakakibara, A.; Suzuki, T. *Chem. Rev.* **1995**, *95*, 1409.
(59) Carley, J. F. *Polym. Eng. Sci.* **1985**, *25*, 1017.
(60) Madbouly, S. A. *J. Macromol. Sci., Part B: Phys.* **2003**, *B42*, 1209.
(61) Utracki, L. A.; Kamal, M. R. *Polym. Eng. Sci.* **1982**, *22*, 63.

MA070186N